Design and Test of an Antenna Module Mock-Up for the EAST 4.6 GHz LHCD Launcher

Design and Test of an Antenna Module Mock-Up for the EAST 4.6 GHz LHCD Launcher*

JIA Hua (贾华), LIU Fukun (刘甫坤), LIU Liang (刘亮), CHENG Min (程敏),
ZHAO Lianmin (赵连敏), WANG Xiaojie (王晓洁), SHAN Jiafang (单家方)

Institute of Plasma Physics, Chinese Academy of Sciences, Hefei 230031, China

Abstract The launcher of the 4.6 GHz lower hybrid current drive (LHCD) system for the Experimental Advanced Superconducting Tokamak (EAST) consists of 24 antenna modules, each composed of an array of 3 (row) × 8 (column) waveguides. In order to verify the radio frequency (RF) design and the feasibility of the manufacturing process, a mock-up of the module has been fabricated and measured. The measured return losses of all three input waveguides are less than −25 dB at a frequency of 4.6 GHz. The transmission coefficients from the input waveguide to the output waveguides are -9.13 ± 0.2 dB and the insertion loss is 0.104 dB. These good results mean that the design method of the antenna module can be used for the new 4.6 GHz launcher on EAST. The detailed design of the multi-junction antenna module and its initial test result are described in this paper.

Keywords: EAST, launcher, lower hybrid current drive

PACS: 52.50.Sw

DOI: 10.1088/1009-0630/15/8/23

1 Introduction

LHCD is an efficient tool to sustain off-axis non-inductive current drive and to maintain steady state currents [1,2] on tokamaks. As a medium sized non-circular cross section superconducting tokamak, EAST aims at performing high parameter discharges and steady-state operations. To meet its experimental requirements, a new 4.6 GHz 6 MW LHCD system is under development. The transmitter is based on 24 VKC-7849A klystrons, each one delivering 250 kW with a 1 dB bandwidth of 8 MHz. All of these klystrons, made by Communications & Power Industries (CPI), can be operated in continuous wave (CW) mode. The VKC-7849A is an upgrade of the pulsed klystron used at Alcator C-MOD. Meanwhile a new launcher, composed of 24 antenna modules, has been designed to inject 6 MW for a pulse length up to 1000 s. The structure of antenna modules is very complicated, because each of them is made of several pieces of metal plates and dozens of metal strips that need to be joined together by brazing. To reduce the risk of design and manufacturing process, it is necessary to build a module mock-up in advance.

During the past 20 years, several kinds of launchers, including the conventional grill, the multi-junction launcher and the passive-active multi-junction (PAM) launcher, have been proposed and used in different tokamaks [3~6]. For EAST the multi-junction launcher is adopted for its compact structure and good coupling property with the plasma.

2 Antenna description

The 4.6 GHz multi-junction launcher is made of 24 antenna modules arranged on 4 rows of 6 columns, as shown in Fig. 1. Each module, fed by one klystron through a TE10-TE30 mode converter/power splitter dividing the power into 3 waveguides, has 3 waveguide rows in the poloidal direction. The waveguide in each row of a module is separated into 8 narrow active waveguides in the toroidal direction by means of 7 E-plane bi-junctions. For the assembly of the launcher, three passive waveguides arranged in a column are inserted between each antenna module in the toroidal direction, each one with a depth of a quarter of the guide wavelength. In addition, a full passive waveguide is mounted on each side of each waveguide row of the launcher. Consequently, the whole launcher is an array of 12 rows of 48 active and 7 passive waveguides.

Fig. 2 is the front view of the rightmost module of a generic row of the launcher, the one on the second row is named the HB1 module. A full passive waveguide is visible on the right side of each row and a half one on the left side. For the inner modules, a half passive waveguide is added on each side, recombining in a full one when the modules are assembled to form the launcher. Water cooling channels are attached on both the top and bottom of each module. The inner structures of the three rows of the HB1 module are shown in Fig. 3. Each row consists of an input waveguide, an E-plane linear taper followed by an oversized waveguide, a set of 7 E-plane waveguide bi-junctions, and phase shifters. The power in each row is divided toroidally into eight sub-

waveguides through these E-plane bi-junctions. The phase difference between the adjacent sub-waveguides is fixed to 90° in the toroidal direction through dozens of built-in stepping phase shifters. Moreover, the phase shifter order after the second bi-junction is $0-\pi-0-\pi$ both in the top and bottom row, but it is $\pi-0-\pi-0$ in the middle row so as to compensate the phase delay in the centre row of the mode converter. The antenna mouth will be finally machined into a curved surface to match the plasma profile, leading to different lengths between waveguide rows. For example, in the HB1 module, the length difference between the top and bottom row is 12.18 mm, corresponding to a poloidal phase difference of 51°. Therefore, to compensate the poloidal length difference, compensating phase shifters are employed for the top and middle row and are computed to have a 0° phase shift between poloidal waveguide rows.
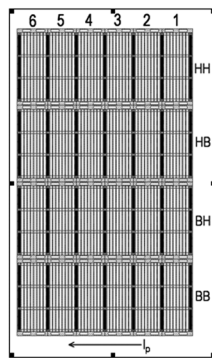

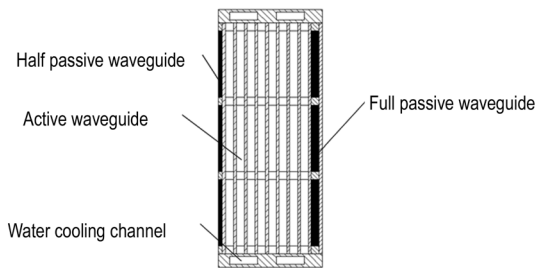**Fig.1** Front view of the configuration of the 6 MW 4.6 GHz LHCD launcher

Fig.2 Front view of the rightmost antenna module of each row of the launcher
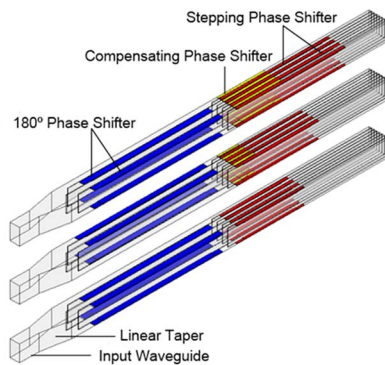

Fig.3 Inner structure of the three rows of the HB1 module (color online)

3 Design of the antenna module

3.1 Design of the sub-waveguides

The RF power is coupled to the plasma directly by the sub-waveguides, whose sizes determine the radiated $n_\parallel$ spectrum of the launcher. Here $n_\parallel$ is the parallel refractive index of the launched wave. If a multi-junction unit, similar to one of the rows of a 4.6 GHz module, is obtained by dividing the main waveguide into several sub-waveguides, the fundamental peak value of the radiated $n_\parallel$ spectrum of the multi-junction units can be written as [7]

$$n_\parallel \approx \frac{c}{\omega \Delta z}\Delta\phi, \qquad (1)$$

where $\triangle z = b + d$, b is the width of the sub-waveguide, d is the septum thickness and $\Delta\phi$ is the phase shift (in radians) between adjacent waveguides. Here, the phases in the sub-waveguides are increasing along with the plasma current, resulting in a spectrum mainly launched in the opposite direction so as to drive the fast electrons.

LHCD experiments require a well defined $n_\parallel$ spectrum. The wave accessibility condition [8], which should be satisfied firstly, is given by

$$n_\parallel \geq N_{\parallel\text{acc}} = \frac{\omega_{\text{pe}}}{\omega_{\text{ce}}} + \sqrt{1 + \frac{\omega_{\text{pe}}^2}{\omega_{\text{ce}}^2} - \frac{\omega_{\text{pi}}^2}{\omega^2}}$$

$$= 3.21\sqrt{n_{\text{e}}}/B + \sqrt{1 + (10.27 n_{\text{e}}/B^2)(1 - (\frac{0.656B}{f\sqrt{M}})^2)}, \qquad (2)$$

where ω_{pe} and ω_{ce} are the electron plasma frequency and electron cyclotron frequency respectively. However, the $n_\parallel$ values of the main peak of the launched spectrum should not be too high, as it will lead to electron Landau damping or mode conversion to the hot ion plasma wave branch in the outer layers of the plasma and will decrease the current drive efficiency. The previous experimental results [7] have shown that the best $n_\parallel$ values of the spectrum are concentrated at low values lying above the limit defined by the wave accessibility to the central region of the plasma. For the EAST physical parameters, $B = 3.5$ T, $f = 4.6$ GHz, the atomic number of hydrogen $M = 1$, and the density in the plasma centre $n_{\text{e}} = 0.5 \times 10^{20}$ m^{-3}, thus the accessible $N_{\parallel\text{acc}} = 1.80$ is obtained from Eq. (2).

For the antenna module, the cross section dimensions of the active sub-waveguides, as well as the passive waveguides, are chosen as 50 mm×6 mm. The septum thickness is 2 mm inside the module and 2.5 mm outside. The phase shift is 90° and the septum thickness between different rows is 6 mm. As calculated from Eq. (1), the antenna module will radiate a power spectrum peaked at $n_\parallel = 2.04$, which is larger than $N_{\parallel\text{acc}} = 1.80$ because the toroidal magnetic field intensity B is lower than the design value most of the time, implying that a relatively larger $n_\parallel$ is needed.

The phase shift between each antenna module can be adjusted by a 6-digit low power electronic phase shifter,

which can change the input phase of the klystron from $0°$ to $360°$ with a step of $5.6°$. The main peak of the radiated spectrum of the launcher can be adjusted from $n_\parallel = 1.79$ to $n_\parallel = 2.23$ when the phase shift between adjacent modules on the same row varies from $0°$ to $180°$. Due to the passive waveguides, the main peak $n_\parallel = 2.04$ will be obtained when the phase shift is set to the default phase of $90°$.

The calculated insertion loss of all the RF components on the transmission line is lower than 1.5 dB and the power density in the module is less than 2.43 kW/cm^2, which is below the weak conditioning region [9]. The maximum electrical amplitude is 2.25×10^5 V/m at the antenna mouth for the forward wave and therefore full power injection ability could be expected.

3.2　Taper section

The taper is used to connect the input waveguide (50 mm×29.1 mm) to the oversized waveguide, whose cross section sizes is 50 mm (height)×62 mm (width). Instead of a stepped impedance transformer, an E-plane linear taper is chosen to reduce the electric field increase at the edges of steps. The linear taper of 84 mm in length is optimized by using the High Frequency Structure Simulator (HFSS) package [10], based on the finite element method. The return loss is less than −33 dB and the maximum electric field amplitude at the input waveguide is 3.6×10^5 V/m. Due to the cross section dimension of the output oversized waveguide and the frequency we use, the generated high order unwanted modes should be suppressed. In the calculation, only the fundamental mode (TE$_{10}$) is considered for the input waveguide, but for the output waveguide, the three propagating high order modes (TE$_{01}$, TE$_{11}$, and TM$_{11}$ mode) are also taken into account besides the TE$_{10}$ mode. The simulation results show that all the three high order modes are dampened to less than −50 dB over a bandwidth of 400 MHz around 4.6 GHz.

3.3　E-plane bi-junctions

The incident power in the main waveguide is divided into 8 sub-waveguides by using a series of E-plane bi-junctions, as shown in Fig. 4. The wave will be reflected by the dividing wall of the bi-junction, where the reflection coefficient is determined by the septum width and waveguide sizes. To reduce the reflected power, the length difference between the first bi-junction and the two second ones is designed to have an electrical length of $90°$. With this configuration, the reflected waves from the two second bi-junctions can be partially cancelled by the one from the first bi-junction [11], because their phase is delayed by $180°$ compared to the latter one. In the 4.6 GHz antenna module, due to the edge effect of discontinuities of the dividing walls, the length difference is designed to be 20.5 mm, which is a little shorter than a quarter guide wavelength.
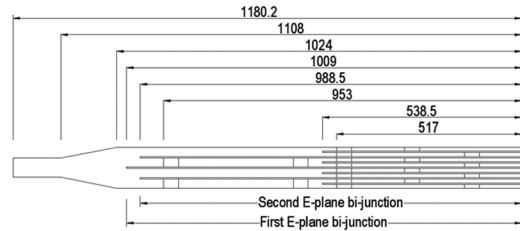
Fig.4 Schematic drawing of the bi-junctions of the antenna module

The lengths of the third bi-junctions are optimized for the coupling by computing the average reflection coefficient R in the input waveguides and the power directivity D_p of the power spectra. Both the effects of plasma load and passive waveguides have been taken into account. For electron density $n_\mathrm{e} = 1.2\times10^{12}$ cm^{-3} and density gradient $\bigtriangledown n_\mathrm{e} = 1.2\times10^{12}$ cm^{-4}, the D_p remains at 75% and R remains below 1% when the phase shift between modules varies from $0°$ to $180°$. Also, the lengths of the second bi-junctions are optimized for low return losses of the input waveguides using HFSS.

The final dimensions for the module are shown in Fig. 4. Here, the length of the oversized waveguide is 15 mm, the length from the first bi-junction to the third ones is 470.5 mm, the length of the third bi-junction is 538.5 mm, and finally, the overall length of the antenna module is 1180.2 mm. When these bi-junctions are being optimized with HFSS, the phase shifters are not added in the simulation, but their lengths have been considered so that the E-plane bi-junctions are long enough to accomodate the phase shifters.

3.4　Phase shifter

The phase shifters are fixed and nonadjustable in the E-plane bi-junctions. Before the launcher installation, the antenna mouth will be machined into a curved surface with a radius of 760 mm in the poloidal and 1968 mm in the toroidal direction. As mentioned before, this will lead to different lengths between waveguides both in the poloidal and toroidal direction and thus produce additional electrical lengths for the waves.

In the toroidal direction, the maximum electrical length difference between neighboring modules is $21.5°$, and only $3.5°$ between neighboring sub-waveguides. For the former this difference can be calibrated out by changing the phases of the antenna modules. While for the latter, we will neglect this difference because it is much less than the phase error resulting from the manufacture tolerance. As a result, the phase difference between adjacent waveguides is designed to be $90°$ in the toroidal direction. With the simplification of neglecting the length differences between neighboring sub-waveguides, the structures of the modules in one row will be the same and thus the manufacture of the launcher will be much easier.

In the poloidal direction instead, the additional electrical length of the three rows facing the plasma surface should be considered. Due to both the $180°$ phase delay

in the middle row of the mode converter and the curvature of the antenna mouth, the poloidal phase difference is fixed and can not be changed once the launcher is completed. For instance, the maximum phase differences resulting from length differences between different rows are 160.5° and 51° in the HH and HB modules respectively. On the other hand, in the 1-dimensional coupling theory, the waveguides are usually assumed as infinitely high and the fields without spatial variation are in the poloidal direction. Consequently, the theoretical analysis of a launcher consisting of multi-row waveguides is identical to that for single row waveguide arrays. In order to make the perpendicular refractive index values of the spectrum in the poloidal direction as low as possible [12] (close to 0), the poloidal phase difference between two vertical sub-waveguides is designed to be 0°, and correspondingly, the phases of the incident waves in different waveguide rows will be identical.

In the antenna module, the compensating and stepping phase shifters are used to countervail the above additional electrical length. They are computed to have a 90° phase shift in the toroidal and 0° in the poloidal directions between neighboring waveguides. The required values of the phase shifters in the third bi-junctions for the HB1 module are computed and listed in Table 1. The shadow in the table means that the π shifters should be put in the waveguides after the second E-plane bi-junctions.

Table 1. Computed values for the phase shifters in the sub-waveguides

	No.8	No.7	No.6	No.5	No.4	No.3	No.2	No.1
Row 1	141	51	141	51	141	51	141	51
Row 2	108	18	108	18	108	18	108	18
Row 3	90.0	0.0	90.0	0.0	90.0	0.0	90.0	0.0

The fixed phase shifter is made by adding two steps in the straight waveguide and thus reducing the height of the waveguide, as shown in Fig. 5. If λ_1, λ_2, λ_g are defined respectively as the guided wavelength of the fundamental mode at the first step region, at the second step region, and at the input waveguide with a height of 50 mm, then the design equation of the fixed shifter can be written as

$$\frac{2\pi}{\lambda_1}2y + \frac{2\pi}{\lambda_2}x - \frac{2\pi}{\lambda_g}(2y + x) = -\phi, \qquad (3)$$

where ϕ is the phase to be shifted, y is the length of the first step and x is the length after the second step. As usual, the quarter wave transformer is used to cancel out the reflected waves from the cut steps, leading to $y = \lambda_1/4$. From Eq. (3), it can be deduced that using the large cut depth can shorten the length of the shifter, but it may cause arcing for high power transmission. With the optimization for minimizing the return loss of the cut step, the parameters for all the phase shifters are chosen as follows: the first cut depth

is 1.75 mm, the second one is 1.25 mm, $y = 22.3$ mm, and the waveguide height of the region after the second step is 44 mm. Then the phase ϕ is dependent only on the length of the region after the second step, namely x. For different phase shifters, the lengths optimized by HFSS are listed in Table 2. These results are very close to the theoretical values that are obtained from Eq. (3). The return losses of all the phase shifters are less than −40 dB in a bandwidth of 200 MHz centered at 4.6 GHz.
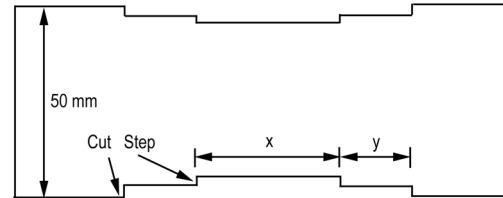

Fig.5 Schematic drawing of a phase shifter with two cut steps

Table 2. Phase shifter lengths from HFSS and in theory for different phases

Phase ϕ (°)	x (mm)	x (mm) in theory
18	11.4	13.79
51	80.4	82.75
90	161.4	164.26
108	199.4	201.88
141	268.4	270.85
180	348.4	352.35

4　RF test result

Fig. 6 shows the HFSS result for the return losses S_{11} of the three input waveguides of the HB1 module. It is seen that the S_{11} parameters of all the input waveguides are less than −25 dB in a bandwidth of 50 MHz. In addition, the calculated power transmission coefficients from the input waveguide to the output waveguides on each row are -9.03 ± 0.1 dB, and the maximum phase difference deviation from 90° of the sub-waveguides is 0.5°.

In order to verify the RF design, a mock-up of the HB1 module has been fabricated, but no water cooling pipes or passive waveguides are added because the RF performance of the antenna module is not being affected. The mock-up is composed of 32 metal strips and 9 metal plates. The phase shifters with steps are machined on these strips, whereas the septa for bi-junctions are made of thin metal plates (the thickness is only 2 mm) with different lengths, both of them made of oxygen-free high-conductivity copper. In particular, the two external plates (5 mm thick) of the module are made of two layers: stainless steel and copper, linked by explosive bonding. When assembled, one metal plate and four strips are stacked layer by layer, fastened with bolts, and finally joined by vacuum brazing to ensure the electrical contact. As a consequence,

different lengths in metal plates lead to different locations of the bi-junctions (see Fig. 3), whereas the sub-waveguides and oversized waveguides are formed in the space between the strips and plates. The linear tapers are inserted into the area of oversized waveguides before the bi-junctions and also fastened to the external metal plates with bolts.
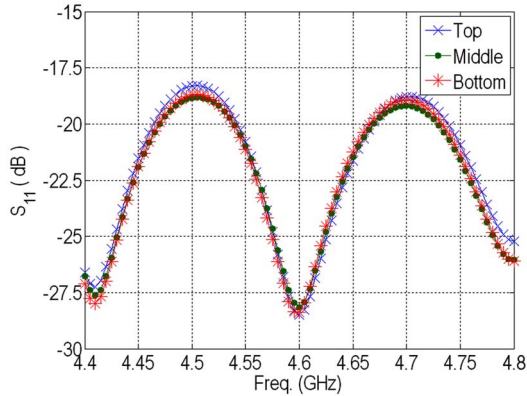

Fig.6 Calculated return losses versus the frequency for all the three input waveguides of the antenna module (color online)

Two impedance transformers have also been made for testing this antenna module mock-up. The first one converts a standard WR229 waveguide to the input waveguide of 50 mm×29.1 mm, and the second one transforms the sub-waveguide (50 mm×6 mm) into a standard WR229 waveguide. Besides, a vector network analyzer Agilent E5071B, two waveguide to coaxial cable transitions, phase stable cables and several home-made wedge loads are also used for the RF test. When the mock-up is being measured, the first transformer is fastened to the input waveguide with bolts, whereas the second one is inserted tightly into the sub-waveguide. The test system of the mock-up is shown in Fig. 7. Note that the three rows of waveguides in the module are tested separately one by one.

Fig.7 RF test system of the antenna module mock-up (color online)

The measurement result indicates that the S_{11} parameters of all the three input waveguides are lower than −25 dB at the frequency of 4.6 GHz. Fig. 8 shows the return loss of the input waveguide and the transmission coefficient from the input waveguide to waveguide No. 5 for the middle row. It can be seen that the values of S_{11} within the frequency range from 4.55 GHz to

4.75 GHz are close to those of HFSS simulation. The slight difference between the calculation and measurement is due to the mechanical tolerances of connections, because when the second transformer is inserted into the sub-waveguide, the electrical contact between them is not good.
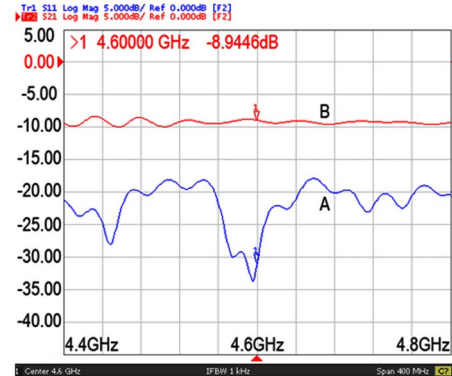

Fig.8 Measured return loss of the input waveguide (A) and the transmission coefficient from the input waveguide to waveguide No.5 (B) for the middle row (color online)
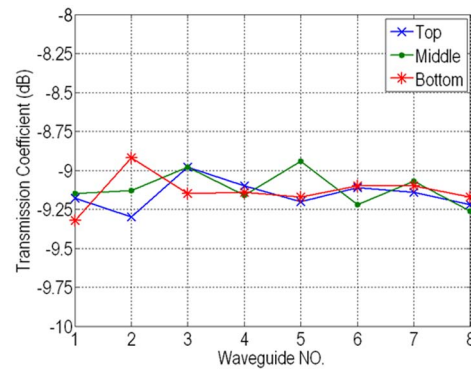

Fig.9 Measured power transmission coefficients from the input waveguide to the 8 sub-waveguides for the three rows (color online)

Fig. 9 shows all the measured power transmission coefficients from the input waveguide to the 8 sub-waveguides for the three rows, and the power attenuation can also be obtained from the measurement results. The measured transmission coefficients are −9.13 ± 0.2 dB, suggesting that the power is almost distributed equally among the sub-waveguides. Moreover, the measured insertion loss for this mock-up is 0.104 dB, meaning that 2.36% of the power is lost due to the conduction loss of copper material. As seen from Fig. 10, the phase shift of 90° between neighboring waveguides in the toroidal direction is confirmed. The maximum phase error is 11° because of the deformation of one copper plates during the welding. One may note that the measured phase values in the middle row are 180° delayed when compared with those in the bottom row, this is because we did not add the $TE_{10}-TE_{30}$ mode converter before the antenna module. Once the phase in the middle row of the mode converter is taken into account, the measured result will be close to the expected values in Table 1.
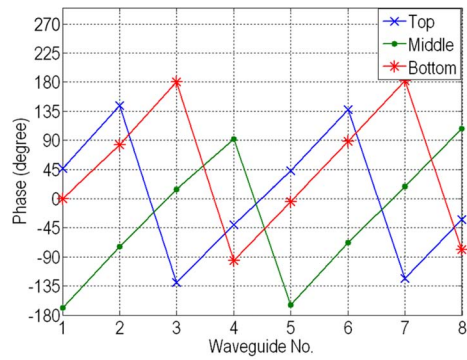
Fig.10 Measured phases for all the 24 output waveguides in three rows (color online)

5 Conclusion

A multi-junction antenna mock-up of the EAST 4.6 GHz LHCD launcher has been realized and tested at low RF power. The measured results are in good agreement with the simulated results, which proves that the design method and manufacture process are reasonable and able to meet the requirements of the EAST 4.6 GHz LHCD launcher. In the near future, a high power level RF test of the antenna module will be carried on at 250 kW for pulse length up to 1000 s. Furthermore, the manufacture of the launcher will be completed by the end of 2012 and the 4.6 GHz LHCD system will be commissioned from the middle of 2013.

References

1 Fisch N J, Karney C F F. 1985, Phys. Rev. Lett., 54: 897
2 Litaudon X, Arslanbekov R, Hoang G T, et al. 1996, Plasma Phys. Controlled Fusion, 38: 1603
3 Hosea J, Beals D, Beck W, et al. 2005, Fusion Engineering and Design, 74: 479
4 Bibet P, Agarici G, Chantant M. 2000, Fusion Engineering and Design, 51~52: 741
5 Pericoli Ridolfini V, Bibet P, Mirizzi F, et al. 2005, Nucl. Fusion, 45: 1085
6 Preynas M, Ekedahl A, Fedorczak N, et al. 2011, Nucl. Fusion, 51: 023001
7 England A C, Eldridge O C, Knowlton S F, et al. 1989, Nucl. Fusion, 29: 1527
8 Golant V E. 1972, Sov. Phys. Tech. Phys, 16: 1980
9 Bae Y S, Paek C H, Rhee M J, et al. 2003, Fusion Engineering and Design, 65: 569
10 Ansoft Corporation. 3D EM simulation software for RF wireless, packaging, and opto-electronic design using Finite Element Method (FEM). http://www.ansoft.com/products/hf/hfss/
11 Litaudon X, Moreau D. 1990, Nucl. Fusion, 30: 471
12 Qin Y L, Ding B J, Kuang G L, et al. 2010, Chin. Phys. B, 19: 065204